

## The Effect of Power on Inductively Coupled Plasma Parameters

Hawraa H. Marza<sup>1\*a</sup>, Thamir H. Khalaf<sup>1b</sup>

<sup>1</sup>Department of Physics, College of Science, University of Baghdad

<sup>b</sup>E-mail: drthamirhameed@gmail.com

<sup>a\*</sup>Corresponding author: hawraa.hafez1204a@sc.uobaghdad.edu.iq

### Abstract

In this work, we studied the effect of power variation on inductively coupled plasma parameters using numerical simulation. Different values were used for input power (750 W-1500 W), gas temperature 300K, gas pressure (0.02torr), 5 turns of the copper coil and the plasma was produced at radio frequency (RF) 13.56 MHz on the coil above the quartz chamber. For the previous purpose, a computer simulation in two dimensions axisymmetric, based on finite element method, was implemented for argon plasma. Based on the results we were able to obtain plasma with a higher density, which was represented by obtaining the plasma parameters (electron density, electric potential, total power, number density of argon ions, electron temperature, number density of excited argon atoms) where the high density in the generated plasma provides a greater degree in material processing, which increases the efficiency of the system. These results may aid in future research towards the development of more efficient optimization of plasma parameters which are (electron density, electric potential, total power, number density of argon ions, electron temperature, and number density of excited argon atoms).

### Article Info.

#### Keywords:

*Inductively Coupled plasma, COMSOL Multiphysics, simulation, ICP plasma, GEC.*

#### Article history:

*Received: Jun. 26, 2022*

*Accepted: Aug. 15, 2022*

*Published: Sep. 01, 2022*

### 1. Introduction

The two most common methods for producing thermal plasma are direct current (DC) arc discharge and inductively coupled discharge [1-6]. The inductively coupled plasma (ICP) torch ionizes the working gas flowing through the quartz tube using high-frequency induction heating. ICP torch has been widely utilized in various industrial applications, such as powder spheroidization. Due to the ultrahigh temperature of flame-like plasma, the ICP torch has been widely adopted in many industrial fields, such as powder spheroidization, high-temperature clean heat source, and mass spectrometry. The inductively coupled discharge is a complex process that involves the interplay of several physical factors, including flow, temperature, and electromagnetic fields [7]. The internal plasma's physical laws are difficult to deduce. Furthermore, during the discharge, electromagnetic interference has a significant impact on the experimental procedure. To examine the many physical fields in the ICP torch, numerical approaches are required [8]. In this type of device, the use of numerical simulation has become a good tool, which gives the possibility to improve ICP operations, which are expensive as well as difficult to implement in an experiment [9]. J. D. Bukowski et al. (1996) [10] also studied a two-dimensional, axisymmetric fluid model of an inductively coupled plasma, and this model prediction was compared to the experimental measurements of P. A. Miller et al [11] of electron density, electron temperature, and plasma potential. Comparisons between model predictions and experimental measurements were made in argon and chlorine gas discharges. In the present work a simulation of the effect of input power variance on plasma parameters which is (electron density, electron temperature, electric potential,

number density of argon ions, and number density of excited argon atoms) and knowing the effect of the input power to increase the density of the plasma.

## 2. Modeling of inductively coupled plasma

Gaseous Electronics Conference cell (GEC) was used to study plasma discharges, as well as give researchers essential experience to develop plasma diagnostics for use in the manufacture of plasma systems [12]. Low pressure (less than  $10\text{Pa}$ ) and high charge density (more than  $10^{17}\text{ m}^{-3}$ ) are typical operating conditions for discharges. Because low pressure ion bombardment can give a greater degree of anisotropy on the wafer surface, high density plasma sources are attractive [13].

The mathematical explanation for the ICP discharge is the Poisson equation, which displays a balance of particle density (electrons and positive ions). The set of drift equations has been solved and used to obtain the average electron energy and electron density, as shown in the equations [14]:

$$\frac{\partial}{\partial t}(n_e) + \nabla \cdot [-n_e(\mu_e \cdot \mathbf{E}) - D_e \cdot \nabla n_e] = R_e \quad (1)$$

$$\frac{d}{dt}(n_\varepsilon) + \nabla \cdot [-n_\varepsilon(\mu_\varepsilon \cdot \mathbf{E}) - D_\varepsilon \cdot \nabla n_\varepsilon] + (\mathbf{E} \cdot \Gamma_\varepsilon) = R_\varepsilon \quad (2)$$

where  $R_e$  gain or loss of electrons due to reactions and collisions,  $R_\varepsilon$  gain or loss of electron energy due to reactions and collisions,  $n_e$  electron number density,  $\mu_e$  electron mobility,  $D_e$  reduced electron diffusivity,  $n_\varepsilon$  the electron energy density,  $\mu_\varepsilon$  electron energy mobility,  $\Gamma_\varepsilon$  flux of electrons energy due to electric field and diffusion. From the electron mobility, the electron diffusivity, energy mobility, and energy diffusivity are calculated:

$$D_e = \mu_e T_e, \mu_\varepsilon = \left(\frac{5}{3}\right) \mu_e, D_\varepsilon = \mu_\varepsilon T_e \quad (3)$$

The plasma chemistry uses rate coefficients to determine the source coefficients in the aforementioned equations. In the case of rate coefficients, the electron source term is given by:

$$R_e = \sum_{j=1}^M X_j K_j N_n n_e \quad (4)$$

where  $X_j$  is the mole fraction of the target species for reaction,  $K_j$  is the rate coefficient for reaction,  $N_n$  is the total number density of neutral. The electron energy loss is obtained by summing the collisional energy loss overall reactions:

$$R_\varepsilon = \sum_{j=1}^P x_j k_j N_n n_e \Delta\varepsilon_j \quad (5)$$

where  $\Delta\varepsilon_j$  is the energy loss from reaction  $j$ . Poisson's Equation [9]

$$-\nabla \cdot \epsilon_0 \epsilon_r \nabla V = \rho_C \quad (6)$$

$\rho_C$  : the space charge density,  $\epsilon_0$  is the vacuum permittivity,  $\epsilon_r$  is the relative permittivity of Argon,  $V$  is electric potential. Space charge density:

$$\rho_C = q \sum_{k=1}^N Z_k n_k - n_e \quad (7)$$

where  $Z_k$  is the charge of species  $k$ ,  $n_k$  Number Density of Species  $k$ . Cold-plasma approximation for plasma conductivity is:

$$\sigma = \frac{n_e q^2}{m_e(v_e + j\omega)} \quad (8)$$

where  $n_e$  the density of electron,  $q$  the charge of electron,  $m_e$  the mass of the electron,  $v_e$  the frequency of the collision, and  $\omega$  is the angular frequency. The rate coefficients can be computed from cross-section data by the following integral[9]:

$$k_k = \gamma \int_0^\infty \varepsilon \sigma_k(\varepsilon) f(\varepsilon) d\varepsilon \quad (9)$$

$k_k$  is the calculated rate coefficients,  $\gamma = \left(\frac{2q}{m_e}\right)^{\frac{1}{2}}$ ,  $f(\varepsilon)$  is the electron energy distribution function,  $\sigma_k$  is the corresponding collision cross section. The following equation is solved for the mass fraction of each species[9, 14]:

$$\rho_m \frac{d}{dt}(w_k) - \rho_m(\mathbf{u} \cdot \nabla)w_k = \nabla \cdot \mathbf{j}_k + R_k \quad (10)$$

where  $w_k$  is the mass fraction of the species  $k$ ,  $\mathbf{u}$  is the mass averaged fluid velocity vector,  $\rho_m$  is the density of the mixture,  $\mathbf{j}_k$  is the diffusive flux vector of the species  $k$ ,  $R_k$  is the generation rate coefficient for species  $k$ . The induction currents are computed in the frequency domain using the equation below[15]:

$$(j\omega\sigma - \omega^2\epsilon_0)\mathbf{A} + \nabla \times (\mu_0^{-1}\nabla \times \mathbf{A}) = \mathbf{J}_e \quad (11)$$

where  $j$  is the imaginary number [13],

$\omega$  is the angular frequency of the electric source ,

$\sigma$  is the electric conductivity,  $\epsilon_0$  is the vacuum permittivity,  $\mu_0$  is the vacuum permeability,  $\mathbf{J}_e$  is the applied external current.

### 3. Argon collision processes

Because the physics in inductively coupled plasma is so complex, it's always better to start with a simple chemical mechanism when modeling. At low pressures, argon is one of the most straightforward processes to apply as shown in Table 1. Table 2 represents the possibility of the atom returning to the ground state when it hits the wall.

Table 1: Ar gas reaction and collisions [16].

Number of reactions	Formula	Type	( $\Delta\varepsilon(eV)$ )
I.	$e + Ar \Rightarrow e + Ar$	Elastic;	0
II.	$e + Ar \Rightarrow e + Ars$	Excitation;	11.5
III.	$e + Ars \Rightarrow e + Ar$	Super elastic;	-11.5
IV.	$e + Ar \Rightarrow 2e + Ar +$	Ionization;	15.8
V.	$e + Ars \Rightarrow 2e + Ar +$	Ionization;	4.24
VI.	$Ars + Ars \Rightarrow e + Ar + Ar +$	Penning ionization;	-
VII.	$Ars + Ar \Rightarrow Ar + Ar$	Metastable quenching;	-

Table 2: Ar gas reaction and collisions [17].

Number of reactions		Formula	Sticking coefficient
I.		$Ar_s \Rightarrow Ar$	I
II.		$Ar+ \Rightarrow Ar$	I

#### 4. The model and simulation domain

This Configuration Fig.1 (a, b) shows ICP as an axisymmetric cross-section in two dimensions using the program COMSOL Multiphysics software by the numerical method (finite element method). As a result, Fig.1 (a) shows the GEC geometry [18] and Fig.1 (b) shows the results of our simulation work shows a cross-section of GEC ICP reactor geometry consisting of a 5 turns copper coil, plasma volume, torch, dielectrics, and wafer with pedestal. A circular spiral coil is supplied with a 13.56 kHz radio frequency (RF) above the quartz chamber. In this work, the simulation was applied to the configuration at gas temperature 300 K, gas pressure 0.02 torr and different power inputs (750, 1000, 1250, and 1500 W) using argon gas. The diameter of copper coils (width 0.003 mm, height 0.003 mm) and there are five turns of copper coil in the model.

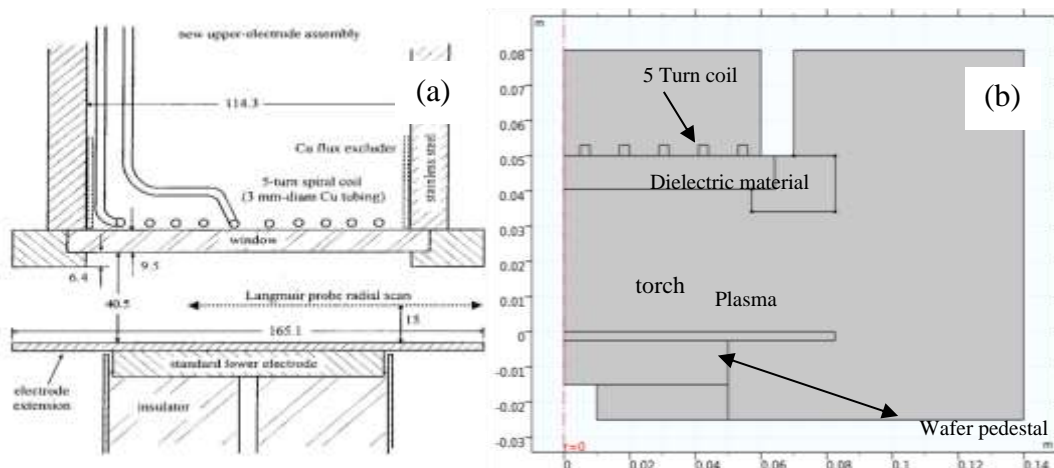
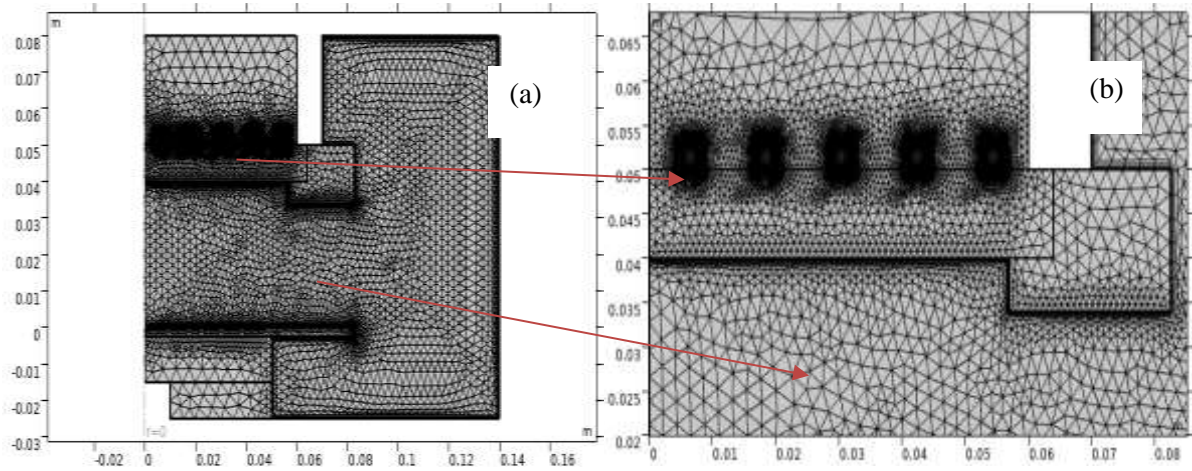


Figure 1: The Simulation domain in two-dimensions, a) the GEC geometry [18] b) cross section of the geometry.

Regarding the calculated precision of the ICP (mesh) model, the arithmetic solution region is divided into small regions of the triangles where the maximum element size is 0.00518 m and the minimum element size is  $1.75 \times 10^{-5}$  m using the finite element method. The process of using the finite element method to translate the configuration equations. In the process of evaluating the solution region in this simulation, both the regions of the plasma torch and coil (of high density) contain more elements than the region that is far from the plasma torch (of low density) because the far regions are not important in the solution. When the same partitioning elements take more time in the implementation, they are in this order to benefit from the time. Fig.2 shows the division of elements in the mesh of the ICP generator in two-dimensional.



**Figure 2:** The domain meshing, a) total mesh, b) enlargement for the region of high-density elements.

## 5. Results and Discussion

### 5.1. Electron Density

The electron density in the plasma medium is one of the most important parameters on which the properties of the plasma depend, so its diagnostics is a priority. Eq. (1) has been solved to find the electron density in the argon plasma under different input powers. Fig.3 shows surface electron density distribution in the cross-section of the cell at different input power values (750, 1000, 1250, and 1500 W). The maximum values ( $7.34 \times 10^{17}$ ,  $9.92 \times 10^{17}$ ,  $1.25 \times 10^{18}$ ,  $1.48 \times 10^{18}$ )  $\text{m}^{-3}$  and the minimum values ( $3.19 \times 10^{14}$ ,  $4.37 \times 10^{14}$ ,  $5.55 \times 10^{14}$ ,  $6.67 \times 10^{14}$ )  $\text{m}^{-3}$ , they found in the densest region inside the ICP plasma, with the increase in the input power, the electron density increases and the plasma torch size increases under the RF coil as shown in the colors of the shape because the degree of ionization increases as the input power increases, the electron density becomes larger.

### 5.2. Electron Temperature

Electron temperature is a form of energy that is important in the plasma because the ionization of plasma is defined by the electron temperature. Therefore, it is one of the most important parameters of plasma and its diagnosis is necessary for plasma operations. Eq. (2) is solved to find the electron temperature in the argon plasma under different input power. Fig.4 shows surface electron temperature distribution in the cross-section of the cell at different input power values (750, 1000, 1250, and 1500W). Since the density of an electron has increased, as in Fig.3, We notice in Fig.4 that the maximum values (3.88,3.87,3.86,3.86) eV and the minimum values (2.24,2.22,2.21,2.21) eV of the temperature of the electron decreases with the increase in input power and the plasma torch size decreases under the RF coil as shown in the colors of the shape. This is due to the increase in the collisions between the electron and the walls of the torch, this means that the rate of the free path will decrease for the electrons, so their temperature will decrease.

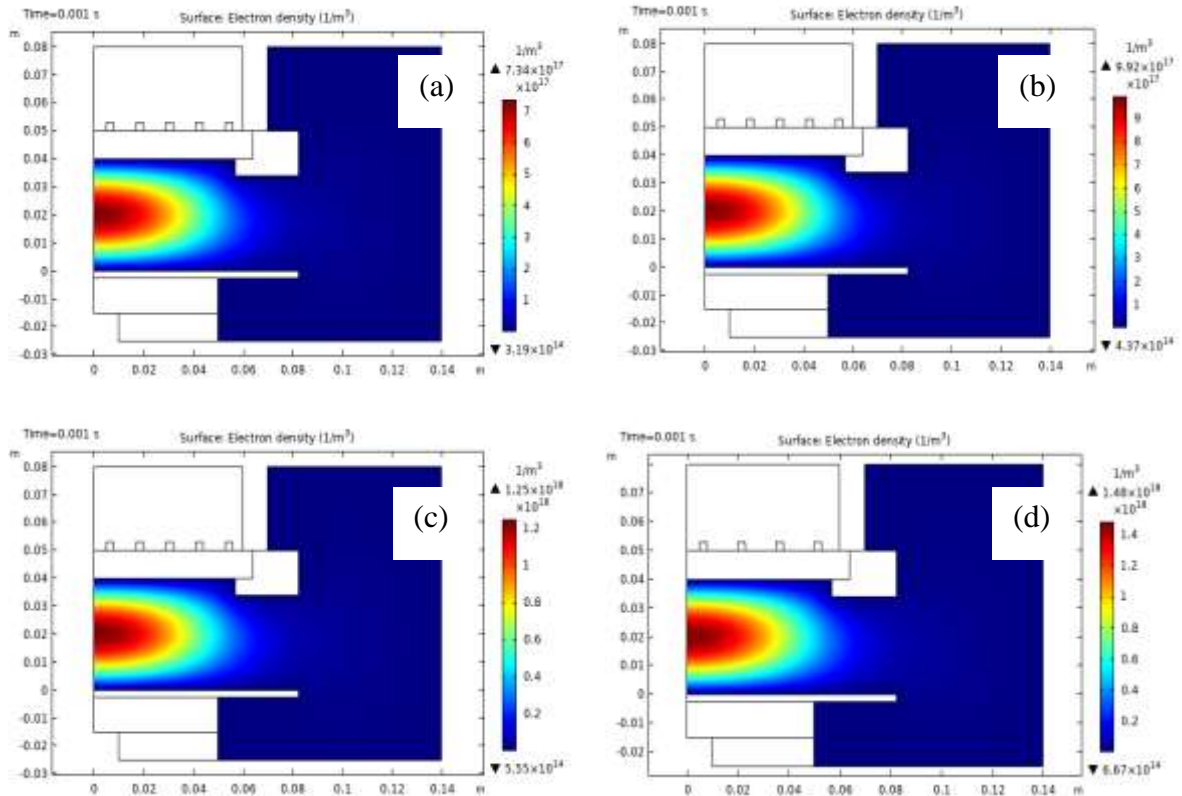


**Figure 3: Electron density distribution at different power value; (a)750W, (b) 1000W, (c) 1250W, (d) 1500W.**

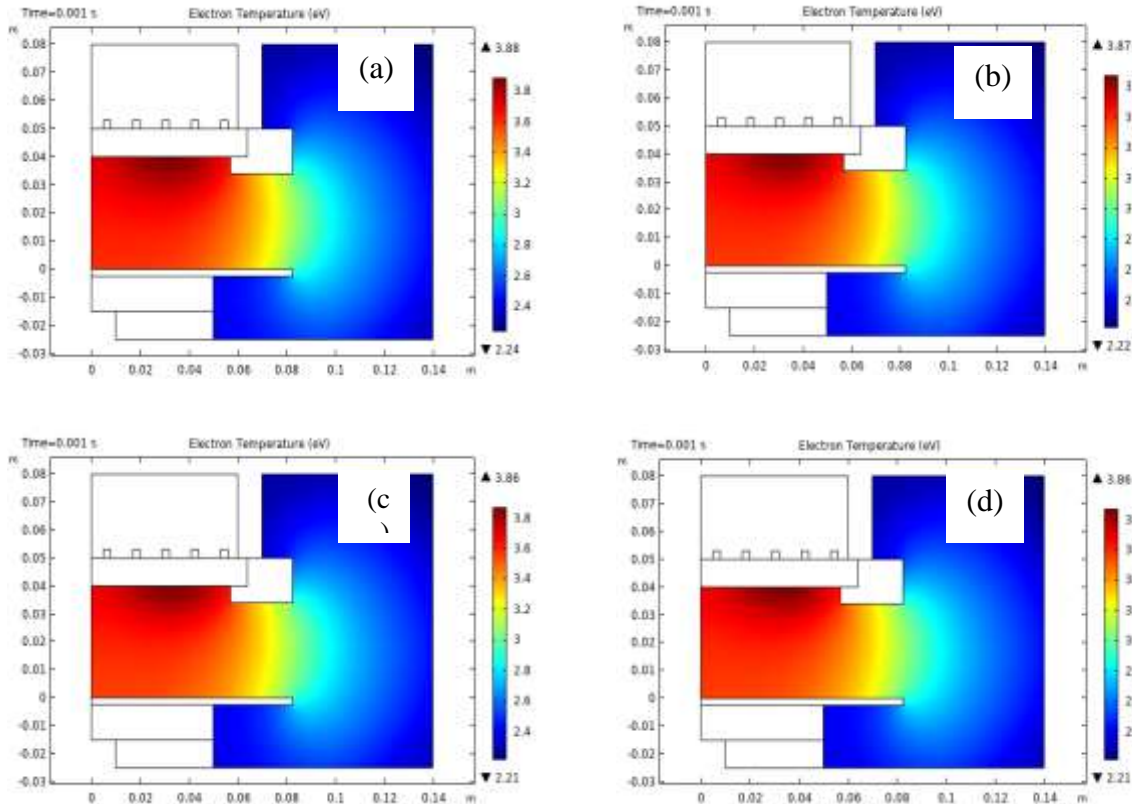


**Figure 4: Electron temperature distribution in (eV) at different power input values; (a)750W, (b) 1000W, (c) 1250W, (d) 1500W.**

### 5.3. Electric Potential

It is one of the main parameters in plasma because the medium of the plasma is a strong connector for electricity. Eq.(6) was solved to find electric potential in the argon plasma under different input power. Fig.5 shows surface electric potential distribution in the cross section of the cell at different input power values (750, 1000, 1250, and 1500W), we notice a decrease in the electric potential at the maximum values (20.3, 20.1, 20, 19.9) V and the minimum values  $(-1.91, -1.97, -1.99, -1.97) \times 10^{-3}V$  with an increase in input power and the plasma torch size decreases under the RF coil as shown in the colors of the shape. This is because the electrical potential of the electrons is lost through collisions (between electrons and atoms inside the chamber and its walls) where electrical energy is converted to other types.

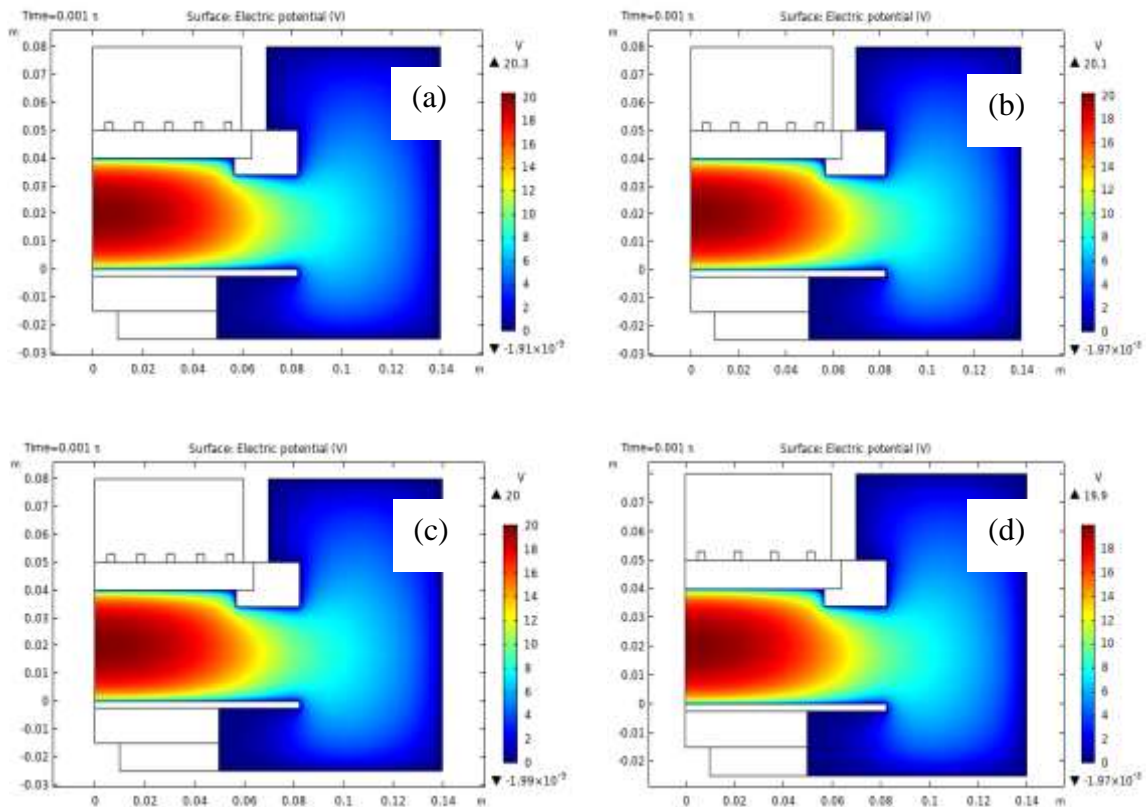


**Figure 5: Electric potential distribution at different power input values; (a)750W, (b) 1000W, (c) 1250W, (d) 1500W.**

### 5.4. Ion Number Density

Since plasma is a semi-ionized medium, where the density of ionized particles is an important factor affecting it and its diagnosis is important. Eq.(7) was solved to find ion number density in the argon plasma under different input power. Fig. 6 shows surface number density distribution in the cross-section of the cell at different input power values. We notice in Fig.6 that when power increases, the density of ions increases and the plasma torch size increases under the RF coil as shown in the colors of the shape, the maximum values of ions density  $(7.34 \times 10^{17}, 9.92 \times 10^{17}, 1.25 \times 10^{18}, 1.48 \times 10^{18}) m^{-3}$  and the minimum values  $(2.87, 4.37, 5.04, 6.67) \times 10^{14} m^{-3}$ . When the power increases, the number of ions and electrons in the torch increases because the degree of ionization increases, and thus causes an increase in the density of ions.

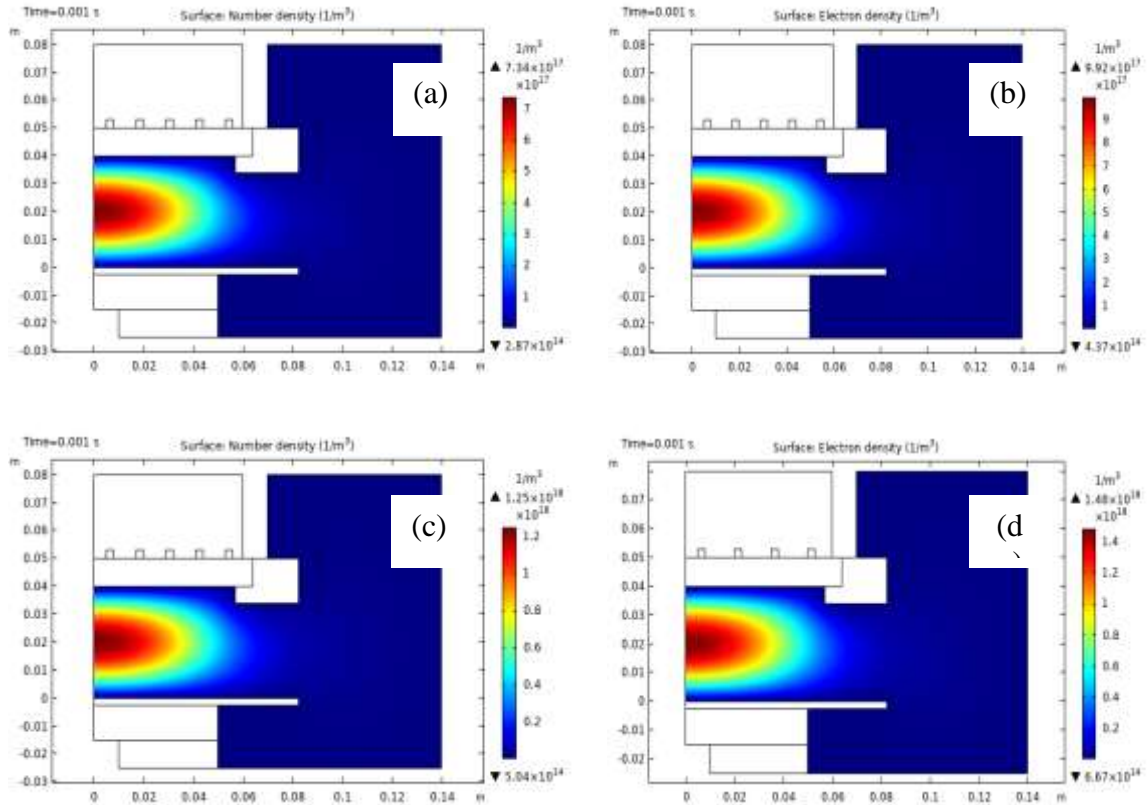


**Figure 6: Ion number density distribution at different power input values; (a)750W, (b) 1000W, (c) 1250W, (d) 1500W.**

### 5.5. Excited Argon Number Density

Eq.(7) was solved to find exciting number density in the argon plasma under different input power. Fig. 7 shows the surface number density of excited argon distribution in the cross section of the cell at different input power values (750, 1000, 1250, and 1500W). It was noted, from Fig. 7, it is clear that an increase in the density of argon gas excited the maximum values were  $8.16, 8.44, 8.62, 8.73 \times 10^{18} \text{ m}^{-3}$  and the minimum values  $(4.18, 3.53, 2.83, 4.76) \times 10^{15} \text{ m}^{-3}$ , the power values increase and the plasma torch size increases under the RF coil as shown in the colors of the shape. This is because the argon atoms will gain energy when increasing the power, which leads to excitation of the atoms, i.e., electrons in the ground energy level will transition to higher energy levels and thus increase the density of excited argon number.

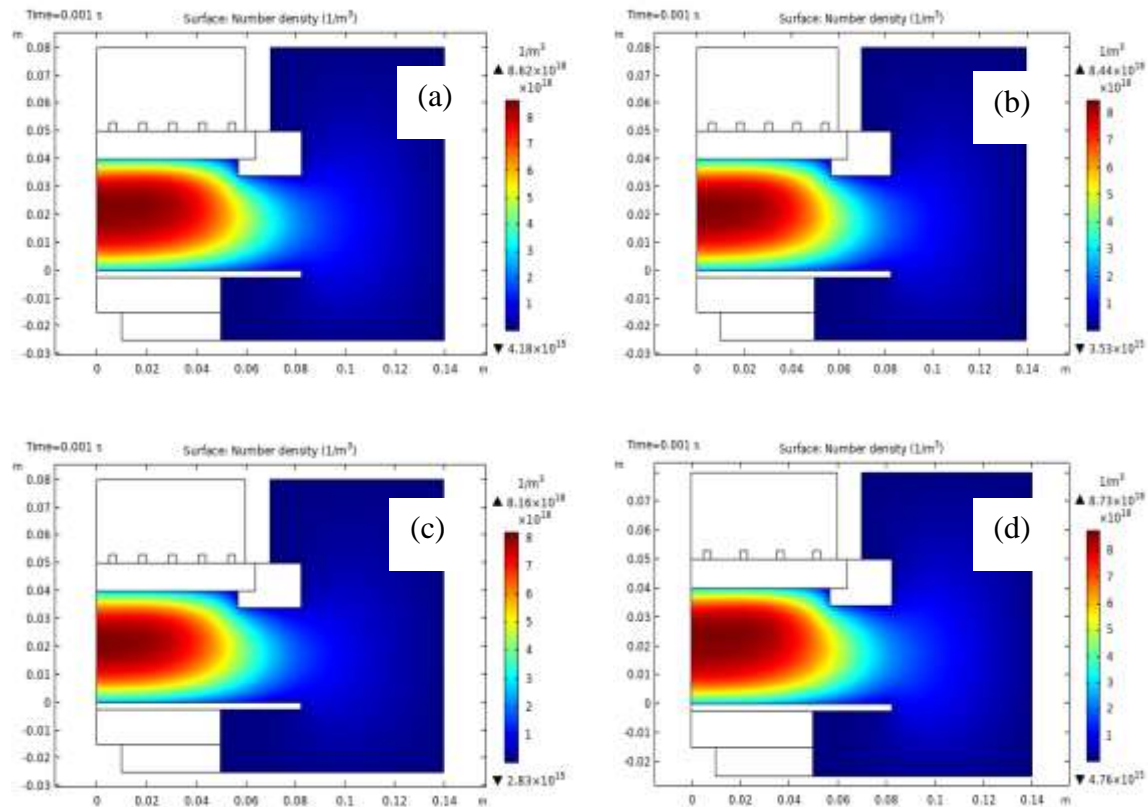


**Figure 7:** Number density distribution at different power input values; (a)750W, (b) 1000W, (c) 1250W, (d) 1500W.

## 6. Conclusion

In recent years, the use of computers, in solving and analyzing scientific problems, has increased because it has the ability to process a lot of data in a short time. The two-dimensional axisymmetric ICP model was studied using COMSOL software with gas pressure (0.02 torr), gas temperature 300K, and different power input (750W-1500W). To gain a better understanding of the dynamics in an argon ICP torch, the electron density, electron temperature, electric potential, number density of argon ions and number density of excited argon atoms were calculated inside argon ICP torch with radio frequency (RF) 13.56 MHz on the coil above the quartz chamber. The change in power values in the ICP torch improves plasma parameters in this simulation, where an increase in electron density, the density of excited argon atoms and number density of argon ions increase the power but the electric potential and electron temperature decrease with an increase in the input power. These results may aid in future research towards the development of a more efficient optimization of plasma parameters.

**Recommendation:** More computational or experimental works can be achieved to study more parameters effects such as (the gas type, the coil type).

## Acknowledgements

The authors would like to thank department of Physics, College of Science, University of Baghdad, Baghdad-Iraq.

**Conflict of interest**

Authors declare that they have no conflict of interest.

**References**

1. Cho D.G., Han J., Han D., and Moon S.Y., *Absolute density measurement of hydrogen atom in inductively coupled Ar/H<sub>2</sub> plasmas using vacuum ultraviolet absorption spectroscopy*. Current Applied Physics, 2020. **20**(4): pp. 550-556.
2. Giersz J., Jankowski K., Ramsza A., and Reszke E., *Microwave-driven inductively coupled plasmas for analytical spectroscopy*. Spectrochimica Acta Part B: Atomic Spectroscopy, 2018. **147**: pp. 51-58.
3. Cai M., Haydar D.A., Montaser A., and Mostaghimi J., *Computer simulation of argon-nitrogen and argon-oxygen inductively coupled plasmas*. Spectrochimica Acta Part B: Atomic Spectroscopy, 1997. **52**(3): pp. 369-386.
4. Deng J., Zhang J., Zhang Q., and Xu S., *Effects of induction coil parameters of plasma torch on the distribution of temperature and flow fields*. Alexandria Engineering Journal, 2021. **60**(1): pp. 501-510.
5. Yin S., *Estimation of rotor position in brushless direct current motor by memory attenuated extended Kalman filter*. European Journal of Electrical Engineering, 2019. **21**(1): pp. 35-42.
6. Gao Y. and Lu H., *A novel Co-planar waveguide-fed direct current wide band printed dipole antenna*. Traitement du Signal, 2019. **36**(3): pp. 253-257.
7. Qin X., Yang G., Cai F., Jiang B., Chen H., Tan C., Kandasamy S.K., Kandasamy K., Sulaiman M., and Su N.C., *Recovery and reuse of spent LiFePO<sub>4</sub> batteries*. J. New Mater. Electrochem. Syst, 2019. **22**(3): pp. 119-124.
8. Meichsner J. and Wegner T., *Evaluation of oxygen species during e-h transition in inductively coupled RF plasmas: combination of experimental results with global model*. The European Physical Journal D, 2018. **72**(5): pp. 1-15.
9. Brezmes A.O. and Breitkopf C., *Fast and reliable simulations of Argon inductively coupled plasma using COMSOL*. Vacuum, 2015. **116**: pp. 65-72.
10. Bukowski J., Graves D., and Vitello P., *Two-dimensional fluid model of an inductively coupled plasma with comparison to experimental spatial profiles*. Journal of Applied Physics, 1996. **80**(5): pp. 2614-2623.
11. Miller P.A., Hebner G.A., Greenberg K.E., Pochan P.D., and Aragon B.P., *An inductively coupled plasma source for the Gaseous electronics conference RF reference cell*. Journal of Research of the National Institute of Standards Technology, 1995. **100**(4): pp. 427-439.
12. Olthoff J.K. and Greenberg K., *The Gaseous electronics conference RF reference cell—An introduction*. Journal of Research of the National Institute of Standards Technology, 1995. **100**(4): pp. 327-339.
13. Lymberopoulos D.P. and Economou D., *Two-dimensional self-consistent radio frequency plasma simulations relevant to the Gaseous electronics conference RF reference cell*. Journal of Research of the National Institute of Standards Technology, 1995. **100**(4): pp. 473-494.
14. Javadvpour S., *Simulation of magnetically confined inductively coupled plasma*, M.Sc. Thesis, South Dakota State University, 2017.
15. Bozkurt E., Güngör Ü.E., and Alemdaroğlu N., *Validation and benchmarking of COMSOL 2D axisymmetric inductively coupled argon plazma model*, 9, Ankara Uluslararası Havacılık ve Uzay Konferansı, AIAC. 2017. pp. 1-12.

16. Bogaerts A. and Gijbels R., *Modeling of metastable Argon atoms in a direct-current glow discharge*. Physical Review A, 1995. **52**(5): pp. 3743-3751.
17. Shirafuji T., Nakamura A., and Tochikubo F., *Numerical simulation of electric double layer in contact with dielectric barrier discharge: Effects of ion transport parameters in liquid*. Japanese Journal of Applied Physics, 2014. **53**(3S2): pp. 03DG04(1-15).

## تأثير القدرة على معاملات البلازما المقترنة حثيًا

حوراء حافظ مرزوه<sup>1</sup>، ثامر حميد خلف<sup>1</sup>  
<sup>1</sup>قسم الفيزياء، كلية العلوم، جامعة بغداد

### الخلاصة

في هذا العمل، درسنا تأثير تغير القدرة على معاملات البلازما المقترنة بالحث باستخدام محاكاة عددية باتجاهين متماثلين. تم استخدام قيم مختلفة لطاقة الإدخال (750 واط - 1500 واط) ودرجة حرارة الغاز (300 كلفن) وضغط الغاز (0.02 تور) و5 لفات الملف النحاسي وتم إنتاج البلازما بتردد راديوي 13.56 ميجا هرتز المسلط على الملف، للغرض السابق، تم تنفيذ محاكاة حاسوبية ذات البعدين، بناءً على طريقة العناصر المحدودة، لبلازما الأرجون. بناءً على النتائج، تمكنا من الحصول على بلازما ذات كثافة أعلى، والتي تمثلت بالحصول على معاملات البلازما (كثافة الإلكترون، الجهد الكهربائي، القدرة الكلية، كثافة عدد أيونات الأرجون، درجة حرارة الإلكترون، كثافة عدد ذرات الأرجون المثارة) حيث توفر الكثافة العالية في البلازما المتولدة درجة أكبر في معالجة المواد مما يزيد من كفاءة النظام. قد تساعد هذه النتائج في البحث المستقبلي من أجل تطوير تحسين أكثر كفاءة لمعاملات البلازما التي هي (كثافة الإلكترون، الجهد الكهربائي، القدرة الكلية، كثافة عدد أيونات الأرجون، درجة حرارة الإلكترون، كثافة عدد ذرات الأرجون المثارة).